

High Temperature Stability of Dispersion Strengthened Copper Alloys Irradiated with Fast Neutrons

DJ Edwards^(a), FA Garner, ML Hamilton, JD Troxell^(b)

OBJECTIVE

The objective of this effort is to further investigate the effects of high temperature neutron irradiation on various GlidCop alloys. The potential for enhancing the performance of the dispersion strengthened copper alloys by additional alloying is also examined.

SUMMARY

Two dispersion strengthened copper alloys, GlidCop CuAl25 and GlidCop-Nb, were irradiated under three different conditions to study their response to high temperature neutron irradiation. Previous studies demonstrated that GlidCop CuAl25 experienced a decrease in yield and ultimate strength by 50 dpa, but no further changes in strength occurred at doses up to 150 dpa. The implications of this are that cold worked (CW) CuAl25 alloys will experience most of the changes in mechanical properties at dose levels that are well within the Basic Physics Phase of ITER's operation. Alloying CuAl25 with 10 wt% Nb produced a DS copper alloy that was completely resistant to any changes in strength during irradiation. These results, when combined with earlier studies, strongly suggest that high temperature neutron irradiation relaxes the dislocation structure within a few dpa (5.8 dpa or less). Alloying with niobium is thought to effectively prevent this relaxation, thereby maintaining the strength of the material.

TECHNICAL PROGRESS

Introduction

The first wall and divertor of ITER require a material with a high thermal conductivity, good strength, and excellent swelling resistance when exposed to neutron irradiation. The high heat flux material will act as a heat sink layer between the beryllium plasma-facing armor and the stainless steel, the latter of which will provide the necessary structural support. Current designs place the operating temperature between 423 and 623 K, with temperature excursions due to plasma disruptions producing an upper temperature limit of 723-773 K for short durations. The operating fluence for the Basic Physics Phase of ITER is currently set at ~3 dpa, while for the Engineering Physics Phase the dose level could reach ~30 dpa.

Dispersion strengthened (DS) copper alloys, commercially known as GlidCop alloys, have been selected over CuNiBe and CuCrZr as the main candidate for the heat sink material. Compared to precipitation hardened alloys such as CuNiBe and CuCrZr, DS copper has the advantage of possessing a high electrical and thermal conductivity that is independent of thermomechanical processing, a characteristic not shared by the precipitation hardened alloys.-

^(a) Post-doctoral Fellow, Associated Western Universities, Richland, WA 99352

^(b) Senior Metallurgist, SCM Metal Products, INC., Triangle Park, NC, 27709-2166

Many of the experiments conducted in the past have tested irradiated DS copper that has been given a series of cold working and annealing treatments. The final state of the material from which specimens were fabricated was often heavily cold worked in spite of the annealing treatments. This cold work leaves the material in a high energy state due to the stored energy, energy that might promote recovery and recrystallization given the enhanced kinetics that occur during irradiation.

The present study investigates the effect of neutron irradiation on the mechanical properties of two heavily cold worked copper alloys, GlidCop-Nb and CuAl25. The GlidCop-Nb alloy represents an attempt to further enhance the strength of GlidCop alloys by adding niobium particles to form a composite structure. The mechanical properties of the irradiated specimens will be compared to those of as-wrought CuAl25.

Experimental Procedure

SCM Metal Products supplied two strips of LOX (low oxygen) grade GlidCop CuAl25 alloyed with 9.6 wt% Nb. The niobium was added to the material by a proprietary process that yields a uniform dispersion of niobium particulates. The alloy also contained ~0.25 wt% aluminum in the form of Al₂O₃ formed by a proprietary internal oxidation process. The GlidCop-Nb alloy contained 200 ppm of boron, which was used to remove any excess oxygen remaining after the internal oxidation process. The GlidCop-Nb strips were 0.254 mm in thickness, and had been given slightly different cold working treatments prior to the final cold working step. The two strips will be referred to as Heat A and Heat B. The final cold work (CW) level for both sheets was 92%.

SCM Metal Products also supplied CuAl25 in the form of 0.254 mm thick strips with a final cold work level of 96%. In addition, GlidCop CuAl25 in the as-wrought condition was used for comparison. The as-wrought material was provided by Dr. B.N Singh at Risø National Laboratory in the form of an as-extruded rod product with a diameter of 12.7 mm. Both materials contained ~250 ppm of boron.

Miniature tensile specimens were fabricated from all four of the materials using an electrical discharge machining process (EDM). Specimens from the GlidCop-Nb were fabricated such that the tensile axis (gage length) of the specimens was parallel to the rolling direction. The specimens from the CW CuAl25 were fabricated in two orientations: with the tensile axis parallel to the rolling direction of the sheet and perpendicular to the rolling direction. Specimens of the as-wrought CuAl25 were fabricated parallel to the extrusion axis of the rod. A schematic of the tensile specimen is given in Figure 1.

Specimens of the two heats of GlidCop-Nb and the CW CuAl25 were irradiated in the Fast Flux Test Facility (FFTF) located in Richland, Washington. The specimens were irradiated at three different locations in FFTF, which lead to specimens being irradiated at three different dose rates. The irradiation conditions are provided in Table 1. All specimens, regardless of location, were in reactor a total of 203 effective full power days. At least 3 specimens of each type of material were irradiated at each set of conditions.

The miniature specimens were tested in a specially designed horizontal testing frame used to test both nonradioactive and radioactive specimens. The specimen was held by wedge grips that have a small square grid on one surface of each grip to improve the grip's ability to clamp and hold the specimen. The load on the specimen was monitored during the tightening of the grips to minimize

any tensile stresses that may be incurred by clamping the specimen. All tensile tests were performed at room temperature using a strain rate of $4 \times 10^{-4} \text{ s}^{-1}$.

Because of the small size and the high residual radioactivity of the irradiated specimens, the strain cannot be directly measured using strain gages. Consequently, the strain is calculated by measuring the crosshead displacement using a linear variable displacement transducer. The displacement is converted to strain by assuming that all of the deformation occurs in the gage section of the tensile specimen. Although the strain values for these miniature specimens may not be directly comparable to that obtained from full size specimens, they can be used to demonstrate major trends in behavior.

The fracture surfaces of individual specimens were examined in a JEOL 840 SEM after testing. The specimens were examined within a few hours of testing in order to minimize oxidation of the exposed fracture surface, which can obscure the surface, especially at high magnifications (>2000x).

Results

The strength of the four unirradiated GlidCop alloys is provided for comparison in Figure 2, along with the room temperature strength measured after irradiation. Note that the two heats of GlidCop-Nb possess the highest yield and ultimate tensile strength (UTS), nearly double that of the unirradiated as-wrought CuAl25. Although it has a similar cold work level, the CW CuAl25 has a noticeably lower strength than the GlidCop-Nb alloys.

The difference in mechanical properties of the two GlidCop-Nb heats is evident in the yield strength, which is ~60 MPa lower for Heat B compared to Heat A. The UTS of these two materials, however, are identical for the unirradiated condition. For the CW CuAl25, the effect of changing the rolling direction in relation to the tensile axis is also evident in the yield strength. The specimens with the rolling direction perpendicular to the tensile axis have an average yield strength ~35 MPa lower than CuAl25 specimens with the rolling direction parallel to the tensile axis. The ultimate tensile strengths are essentially identical.

To further demonstrate the differences in tensile behavior between these three types of alloys, the actual tensile curves from representative specimens are given in Figure 3. The as-wrought material clearly possesses the best ductility, with a total elongation roughly double that of the other three alloys. Note that the elongations of the GlidCop-Nb alloys and the CW CuAl25 are similar despite the differences in strength. Their uniform elongation is around 1.5 to 2%, typical for heavily cold worked GlidCop. Even with a uniform elongation of around 7.5% for the as-wrought CuAl25, none of the alloys exhibit the ability to strain harden significantly.

It is obvious in Figure 2 that the GlidCop-Nb alloys exhibit the best resistance to high temperature neutron irradiation. There is very little change in the UTS of the two heats of GlidCop-Nb, although in the yield strength there is a noticeable decrease. The yield strength decrease is by roughly the same amount for the two higher doses but is slightly less for the specimens irradiated at 643 K to only 5.8 dpa.

Representative tensile curves for the irradiated GlidCop-Nb (Heat B) are shown in Figure 4 for comparison with the unirradiated GlidCop-Nb. The most noticeable effect of irradiation is that the irradiated specimens appear to exhibit slightly more strain hardening ability. Although the tensile curves suggest that the total elongation might be increasing with dose, the differences in the

elongation values of the three curves are not significant.

Of the GlidCop-Nb Heat A specimens irradiated to 34.5 dpa at 706 K, half were found to exhibit an unusual change in the initial plastic region of the tensile curve as illustrated in Figure 5. The reason for the change in the slope of the curve is not apparent. The main effect is to produce a yield strength that is significantly below that of the other Heat A specimens; the UTS was unaffected. The yield strength for these specimens is also shown in Figure 2 /for comparison.

As shown in Figure 2, the CW CuAl25 specimens experienced the largest change in strength with irradiation. The differences in yield strength between the "parallel" and the "perpendicular" specimens are no longer evident after irradiation. The UTS of both types of specimens dropped roughly 150 MPa after irradiation, and was accompanied by an increase in elongation, as shown by the representative tensile curves of the "parallel" specimens provided in Figure 6. The magnitude of the decrease in the UTS was about the same regardless of the irradiation dose and temperature. The same behavior was observed for the yield strength. Note, however, that the yield strength after irradiation was almost the same as that measured for the unirradiated CW CuAl25. Unlike the GlidCop-Nb alloys, the changes in elongation after irradiation are larger, indicating that irradiating to doses higher than 5.8 dpa at higher temperatures produces an increase in both the uniform and total elongation.

One other feature observed in the tensile curves that bears mentioning is that the specimens irradiated to 18.4 and 34.5 dpa exhibited a yield plateau observed in an earlier study by Anderson et al. [1] and Edwards et al. [2]. Figure 7 shows an example of this for the CW CuAl25 irradiated to 18.4 dpa. The cause for this phenomenon has yet to be determined. This is due in part to the fact that the deformed specimens are so small, i.e., the small gage width, coupled with the high radioactivity of the specimens, makes it difficult to obtain useful specimens for transmission electron microscopy (TEM).

Fractography on fracture surfaces from both the GlidCop-Nb and the CuAl25 alloys revealed that the failure mode was microvoid coalescence in both the unirradiated and irradiated specimens. Examples of the fracture surfaces for both alloys are given in Figures 8 and 9. As observed previously by Anderson et al. [1] and Edwards et al. [2], several α -Al₂O₃ inclusions were present inside the dimples. After irradiation these particles were no longer visible on the fracture surface, indicative of a possible change in cohesive strength at the interface between the inclusion and the matrix.

Discussion

DS copper alloys are considered to be extremely stable at high temperatures for short term exposures. However, the influence of displacement rate, temperature, and long term exposure at temperatures near 0.5 T_{mp} (melting temperature) has never been fully elucidated with regard to the effect of these variables on the mechanical properties of this class of alloys. The following discussion provides insight into the possible role that these variables may serve in determining the effect of neutron irradiation on the mechanical properties.

1. CW CuAl25

As noted earlier, the strength of the CW CuAl25 decreased after irradiation to a level slightly above that of the unirradiated as-wrought CuAl25. This decrease was independent of the displacement rate and temperature, suggesting that the changes in the microstructure responsible for

the decrease in strength are complete at relatively low dose levels. Evidence to support this can be obtained by comparing the present results with those of the previous microstructural and mechanical property studies of irradiated GlidCop alloys.

It has been shown in previous work by Edwards and coworkers [1-4] that 50% CW CuAl25 exhibited excellent retention of strength after exposure to neutron irradiation at ~690 K. Although they found that the strength decreased roughly 15% after irradiation to 48 dpa, further irradiation to 104 and 150 dpa did not produce any additional changes in strength. The actual levels of strength achieved in that material were slightly different than that measured for the CW CuAl25 in this study. This can be attributed entirely to the differences in cold working treatments given to the two materials (50% CW vs. 96% CW), which would also affect how the materials responded to the neutron flux. Essentially the higher cold work level would result in more recovery and recrystallization because of the stronger driving force arising from the higher stored energy.

Because the lowest dose available in that study was 48 dpa, it was not clear whether the saturation in strength changes would be reached at lower doses. However, a previous study by Brager et. al. [5] showed that CuAl25 in the 20% cold worked condition also experienced a decrease of ~15% in yield strength after irradiation to 16 dpa at ~703 K. The similarity in the change in yield strength suggests that many of the changes in the microstructure have already occurred by 16 dpa. Note that the displacement rate for both of the earlier studies was $\sim 1.4 \times 10^{-6}$ dpa/sec, comparable to that of the current experiment.

Edwards and coworkers found that the GlidCop alloys irradiated at 690 K experienced varying degrees of recovery and recrystallization dependent upon the volume fraction of Al_2O_3 . The stability of the microstructure at high doses was found to be directly linked to the presence of the small Al_2O_3 particles, typically 7-8 nm in diameter. As the volume fraction of Al_2O_3 increased, the degree of recovery and recrystallization became smaller. For each alloy studied, no further changes in the microstructure were observed after 48 dpa, corresponding directly with the observed saturation in changes in the mechanical properties.

There were some early concerns that the particles might be dissolved by ballistic dissolution, thereby compromising the performance of these alloys under irradiation. As the mechanical property measurements and the microstructural studies revealed, these concerns proved unwarranted. The particle morphology changed under irradiation, as discussed elsewhere [6], but in general the size distribution and number density of the oxide particles remained unaltered. The irradiation stability of the Al_2O_3 particles in GlidCop and other DS copper alloys has also been investigated by Wanderka et al. [7] and by Zinkle et al. [8,9] in other studies, further establishing the resistance of these particles to complete dissolution. The recrystallization observed in the irradiated alloys occurred in regions where the particle density was relatively low. A high density of particles was far more effective at pinning the dislocations, and in such areas the relaxation of the dislocation structure appeared to be limited to recovery. The density limit at which recrystallization was prevented in localized areas was not established in previous studies, and remains an issue that might bear further investigation.

Since it was established in earlier work that the microstructural alterations that coincide with the changes in strength were completed by 48 dpa, and given that the specimens irradiated in this study to 5.8 dpa have basically the same response as the specimens irradiated to 18.4 and 34.5 dpa, it seems likely that the microstructure of the three sets of specimens are very similar. If this is confirmed by transmission electron microscopy, it would lead to the conclusion that the relaxation in the dislocation structure occurs independently of the displacement rate and temperature, at least

within the range investigated in this study (3.3×10^{-7} dpa/sec, 643 K, to 2.0×10^{-6} dpa/sec, 706K). If this is true, then the changes in mechanical properties appear to saturate at doses as low as 5.8 dpa.

It is difficult to separate the effects of neutron irradiation at ~ 673 K from simple annealing effects that occur during the long term exposure at ~ 673 K. The specimens irradiated in this study were in reactor at ~ 673 K for 203 days, or 4900 hours. Anderson et al. [1] reported that annealing 50% CW CuAl25 for 1026 hours at 693 K produced a decrease in strength very similar to that observed for the same material irradiated to 48 dpa at ~ 673 K. Similar behavior was observed for 20% CW CuAl20, indicating that some of the changes in mechanical properties may be thermally induced. One way to clarify this issue is to test specimens that were irradiated to comparatively low doses, less than 0.01 dpa, at a range of temperatures above and below the irradiation hardening regime (< 473 K). The effects of irradiation at low temperatures and at doses low enough to avoid any significant irradiation hardening may show that the dislocation structure can be relaxed by the extra vacancies and interstitials produced during irradiation [10]. Singh and coworkers have found evidence to support this after irradiating heavily cold worked CuAl25 to doses ranging from 0.01 to 0.3 dpa at 323 K [11]. At 0.01 dpa they observed that the yield strength actually decreased $\sim 10\%$, demonstrating that irradiating at temperatures near room temperature lowered the strength due to radiation-induced relaxation of the dislocation structure. Beyond 0.01 dpa the strength began to increase dramatically due to the presence of defect clusters, so any further relaxation in the dislocation structure was masked by the irradiation hardening.

2. GlidCop-Nb Alloys

While the UTS of these alloys changed very little after irradiation, the yield strength showed a significant drop that may be due either to recovery and recrystallization, or to a change in the dispersion of Al_2O_3 particles and niobium particulates. The microstructure of these specimens needs to be examined by TEM to ascertain what changes might be responsible for the drop in yield strength.

The electrical conductivity of this alloy needs to be measured to see if there are any unusual effects related to transmutation. In a previous study by Edwards et al. [4], a Cu-HfO₂ alloy was found to maintain a minimum level of conductivity after irradiation to 50 dpa and beyond. This type of behavior has not been found in any other copper alloy: rather, the conductivity decreases with increasing neutron exposure due to transmutation. Microstructural analysis revealed that after irradiation the original HfO₂ particles were rich in nickel due to transmutant nickel segregating to the HfO₂. It has never been established whether the nickel segregation was the result of a Hf-Ni-O phase, or whether the large incoherent interface of the HfO₂ particles acted as a sink for nickel. If the interface was the controlling factor in the segregation, then finely dispersed niobium-rich particulates might produce the same effect.

3. Fracture Surfaces

The fracture surfaces of all three materials were essentially the same, and indicated that failure occurred as a result of microvoid coalescence. The unirradiated CW CuAl25 had large $\alpha-Al_2O_3$ inclusions present inside some of the dimples on the fracture surface. As noted in a previous study these inclusions were not found on the fracture surfaces of irradiated specimens. Edwards et al. [6] proposed that the reason behind this disappearance was related to the formation of $\eta'-Al_2O_3$ at the interface of the inclusions. Faceted platelets of $\eta'-Al_2O_3$ were observed at the interface of the $\alpha-Al_2O_3$ inclusions, and were presumed to have formed as the result of enrichment of the matrix near

the interface due to ballistic dissolution of the inclusion. If deformation voids formed in the unirradiated specimens at the interface of the inclusions, then the presence of η' - Al_2O_3 platelets might affect how easily voids could form at the interface in the irradiated specimens. The ballistic dissolution referred to here does not refer to the dissolution of the Al_2O_3 dispersoid responsible for the stable dislocation structure, but only to the large micron-sized α - Al_2O_3 inclusions.

4. Transmutation

It was shown recently by Edwards et al. [12] that the nickel and zinc produced by transmutation are responsible for the decrease in electrical conductivity observed in the CuAl25 irradiated at ~ 690 K to doses between 48 and 150 dpa. In previous studies this alloy has never been found to swell due to bubble or void formation, so conductivity changes were attributed exclusively to the nickel and zinc. Density measurements have not been made on the alloys in this study, so it is not known whether any density changes have occurred.

These alloys were all deoxidized using boron, which leaves a residual concentration of ~ 200 ppm of boron (by weight) in the material. This boron will transmute to form helium and lithium by the $^{10}\text{B}(n,\alpha)^7\text{Li}$ reaction. Approximately 25% of the boron in these specimens will be transmuted to helium and lithium. Although the helium to dpa ratio will be different in the three locations used in this experiment, the amount of boron transmutation will be roughly the same regardless of the location. The only swelling data currently available for an irradiated GlidCop alloy containing boron are those of Anderson et al. [1] and Edwards et al. [2-4], which showed that CuAl15 experienced variable swelling during irradiation. The swelling was due to the formation of helium bubbles that formed at or near the oxide particle interfaces. Neither of the other two GlidCop alloys, CuAl20 and CuAl25, contained any boron. The swelling resistance of the CuAl15 might be much less than that of the CuAl25 since it has a lower volume fraction of Al_2O_3 . Density measurements should be conducted on the specimens irradiated in this study to determine whether the higher volume fraction of Al_2O_3 in the CuAl25 can prevent swelling despite the presence of boron.

Conclusions

The GlidCop-Nb alloys exhibit extreme resistance to any degradation in strength. The reason for this is assumed to be related to the presence of a high density of Nb-rich particulates that are very effective at preventing recovery and recrystallization. This assumption must be confirmed by electron microscopy on both the unirradiated and irradiated specimens.

The implications of this study are that the CW CuAl25 alloys will experience most of the changes in mechanical properties at dose levels that are well within the Basic Physics Phase of ITER's operation. It is likely that the changes may even occur at dose levels lower than 1 dpa, however, additional data must be gathered before this is certain. Whether the same kind of behavior will be observed at lower temperatures remains to be determined.

Transmutation effects bear further investigation since it is not known whether the presence of boron will lead to swelling in the CuAl25.

FUTURE WORK

TEM will be performed on both the GlidCop-Nb and CW CuAl25 to investigate the changes that occurred under irradiation. Density measurements and electrical conductivity measurements will

also be made to compare with the results obtained in previous experiments.

ACKNOWLEDGEMENTS

This work was supported by the U.S. Department of Energy Office of Fusion Energy under contract DE-AC06-76RLO 1830. One of the authors (DJ Edwards) would like to thank Dr. B. N. Singh and Risø National Laboratory for supplying the as-wrought CuAl25.

REFERENCES

1. K. R. Anderson, F. A. Garner, M. L. Hamilton, and J. F. Stubbins, *15th International Symposium on the Effects of Irradiation on Materials, ASTM STP 1125*, R. E. Stoller, A. S. Kumar, and D. S. Gelles, Eds., 1992, p. 854.
2. D. J. Edwards, *Ph.D Dissertation*, University of Missouri-Rolla, (1993).
3. D. J. Edwards, J. W. Newkirk, F. A. Garner, M. L. Hamilton, A. Nadkarni, and P. Samal, *15th International Symposium on the Effects of Irradiation on Materials, ASTM STP 1175*, A. S. Kumar, D. S. Gelles, R. K. Nanstad, and E. A. Little, Eds., 1993, p. 1041.
4. D. J. Edwards, K. R. Anderson, F. A. Garner, M. L. Hamilton, J. F. Stubbins, and A. S. Kumar, *J. Nucl. Matls.*, **191-194**, (1992), p. 416.
5. H. R. Brager, H. L. Heinisch, and F. A. Garner, *J. Nucl. Matls.*, **133-134**, (1985), p. 679.
6. D. J. Edwards, F. A. Garner, J. W. Newkirk, and A. Nadkarni, *J. Nucl. Matls.*, **212-215**, (1994), p. 1313.
7. N. Wanderka, Y. Yuan, L. Jiao, R. P. Wahi, and H. Wollenberger, *J. Nucl. Matls.*, **191-194**, p. 1356.
8. S. J. Zinkle, A. Horsewell, B. N. Singh, and W. F. Sommer, *J. Nucl. Matls.*, **195**, (1992), p. 11.
9. S. J. Zinkle, E.V. Nesterova, V. R. Barabash, V. V. Rybin, and A. V. Naberanov, *J. Nucl. Matls.*, **208**, (1994), p. 119.
10. B. N. Singh, *Private communication*, (1995).
11. B. N. Singh, "Assessment of Physical, Mechanical, and Technological Properties of First Candidate Copper Alloys", ITER Assessment Report, (1994).
12. D. J. Edwards, F. A. Garner, and L. R. Greenwood, *J. Nucl. Matls.*, **212-215**, (1994), p. 404.

TABLE 1 Irradiation Conditions for Cold Worked DS GlidCop Alloys

Alloy	Irradiation Temperature (K)	Fluence ($E > 0.1$ MeV)	Total displacement (dpa)	Displacement rate (dpa/sec)
GlidCop-Nb CW CuAl25	643	1.14×10^{22}	5.8	3.3×10^{-7}
GlidCop-Nb CW CuAl25	666	3.3×10^{22}	18.4	1.1×10^{-6}
GlidCop-Nb CW CuAl25	706	6.0×10^{22}	34.5	2.0×10^{-6}

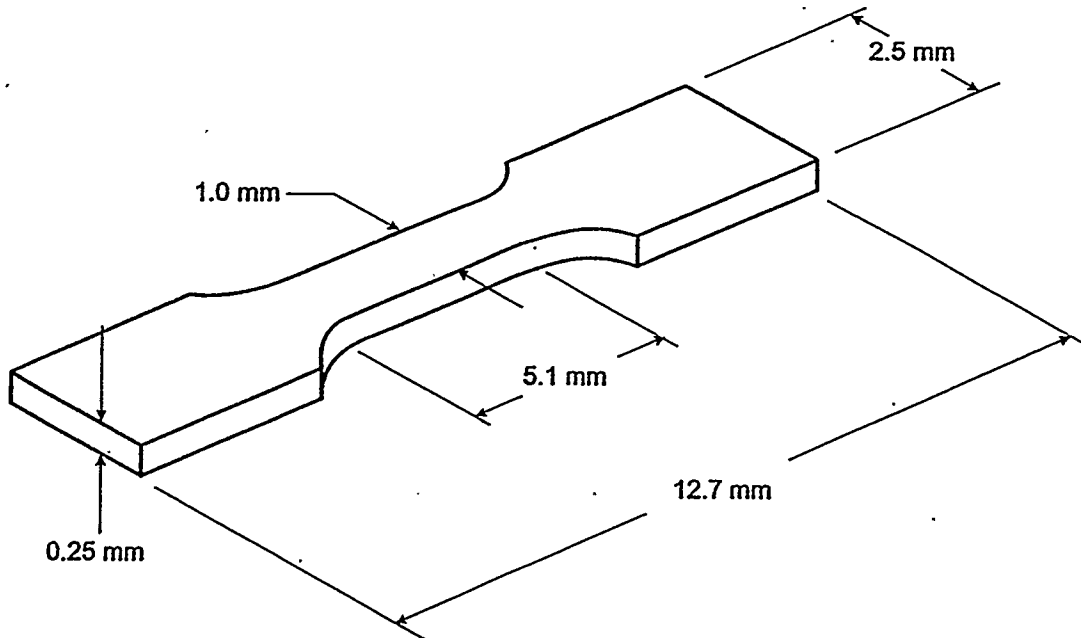
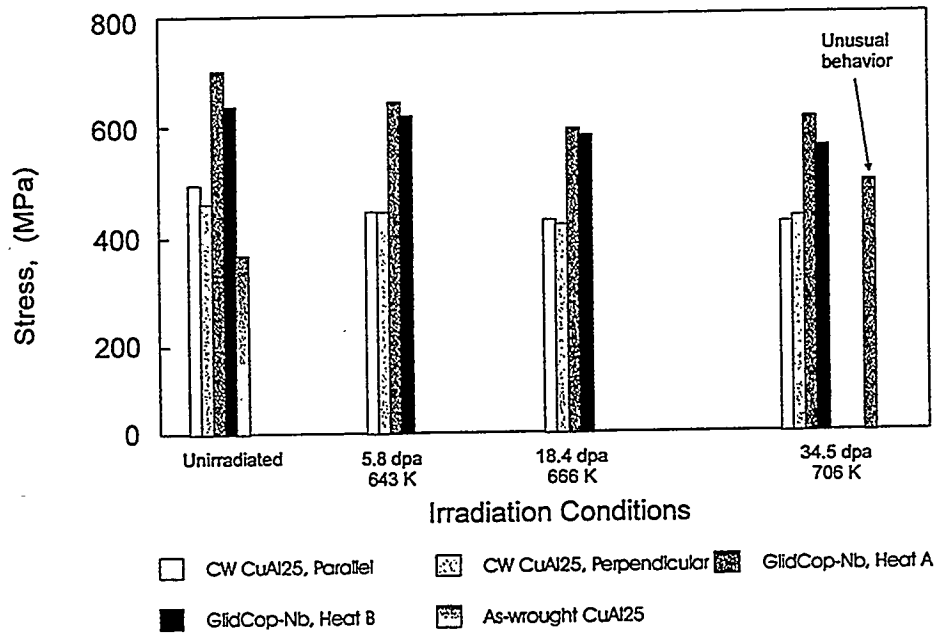


Figure 1. Schematic of the miniaturized tensile specimens.

Yield Strength of GlidCop Alloys



UTS of Irradiated GlidCop Alloys

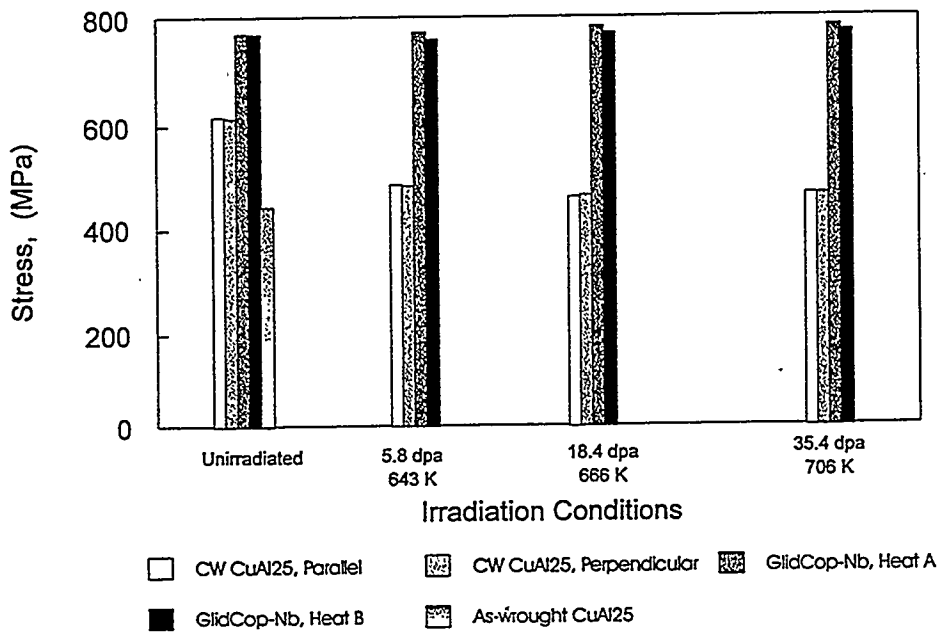


Figure 2. Yield strength (a) and UTS (b) of the unirradiated GlidCop alloys.

Figure 3. Tensile curves of the unirradiated GlidCop alloys.

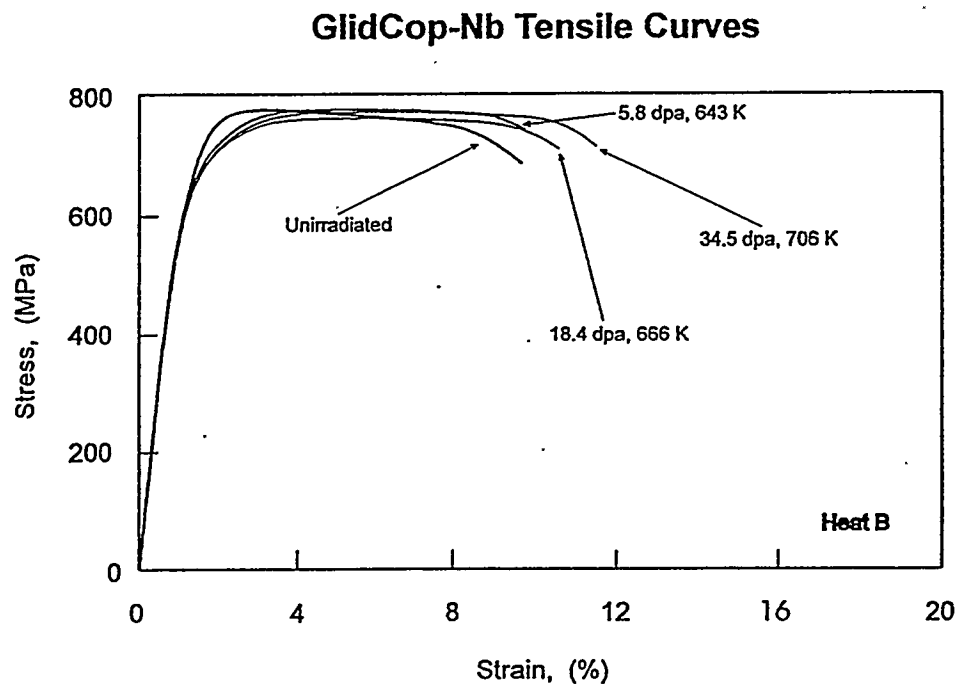
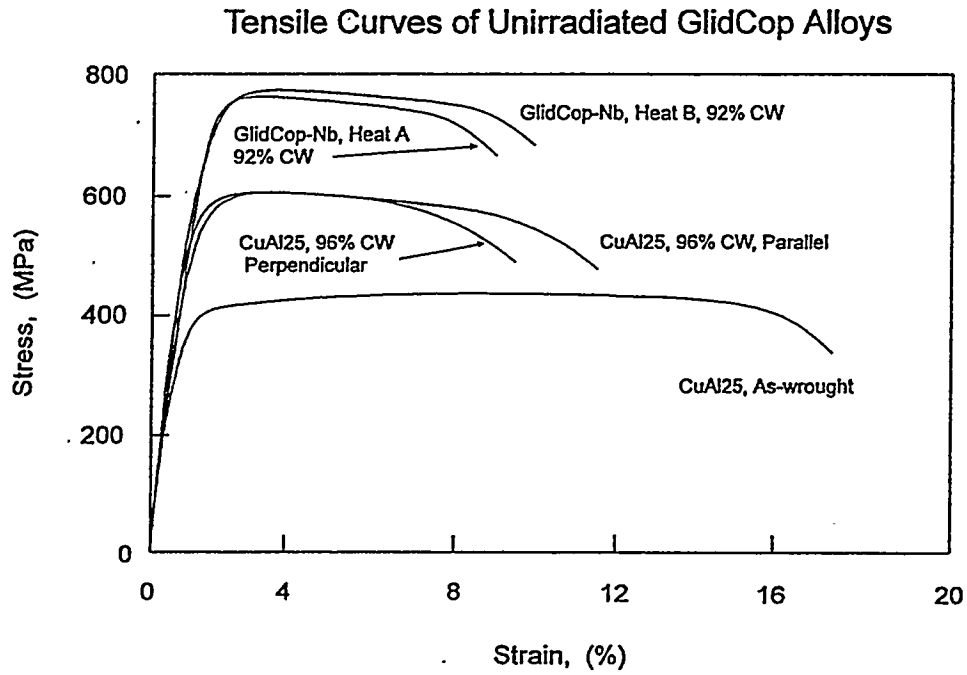


Figure 4. Tensile curves of the unirradiated and irradiated GlidCop-Nb alloys.

Figure 5. Unusual tensile behavior observed in the GlidCop-Nb irradiated to 34.5 dpa at 706K.

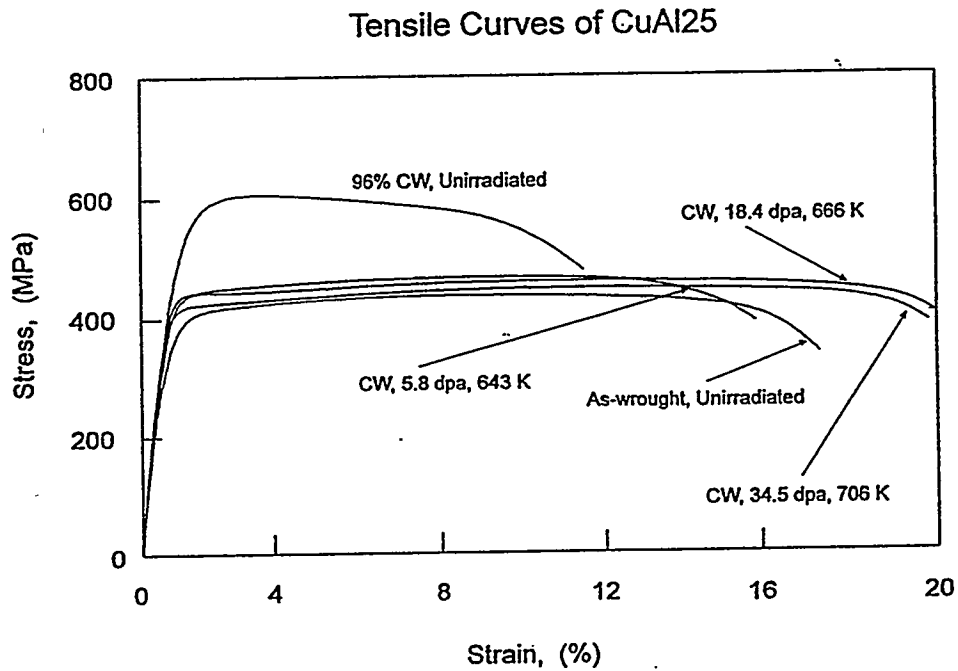
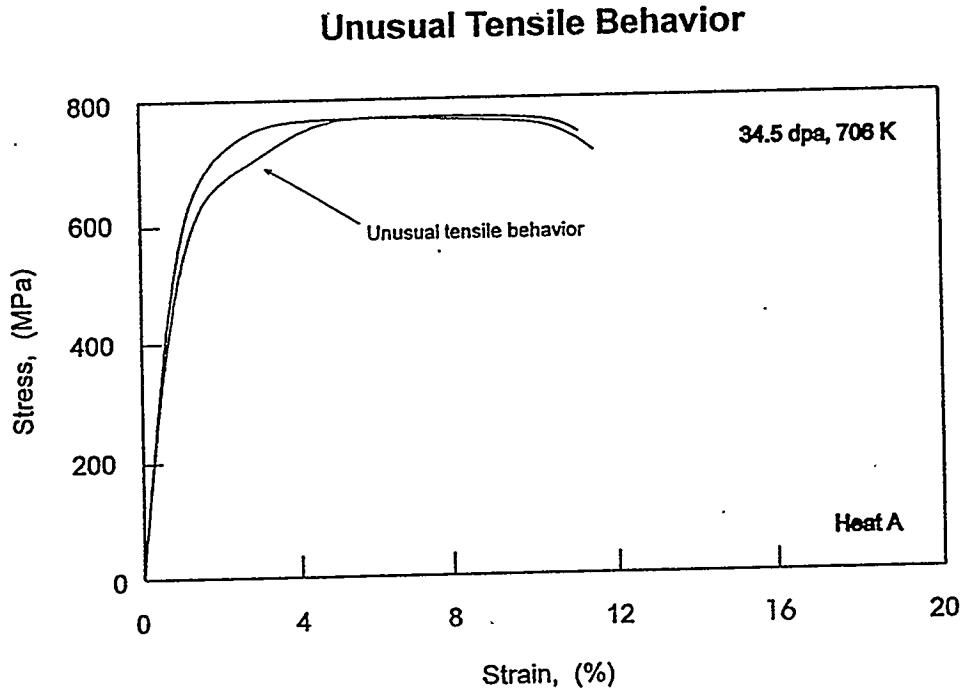


Figure 6. Tensile curves of the unirradiated and irradiated 96% CW CuAl25. A tensile curve for the unirradiated, as-wrought CuAl25 is provided for comparison.

Figure 7. Tensile curve demonstrating the yield plateau observed in this study and the work of Anderson et al. [1] and Edwards et al. [4].

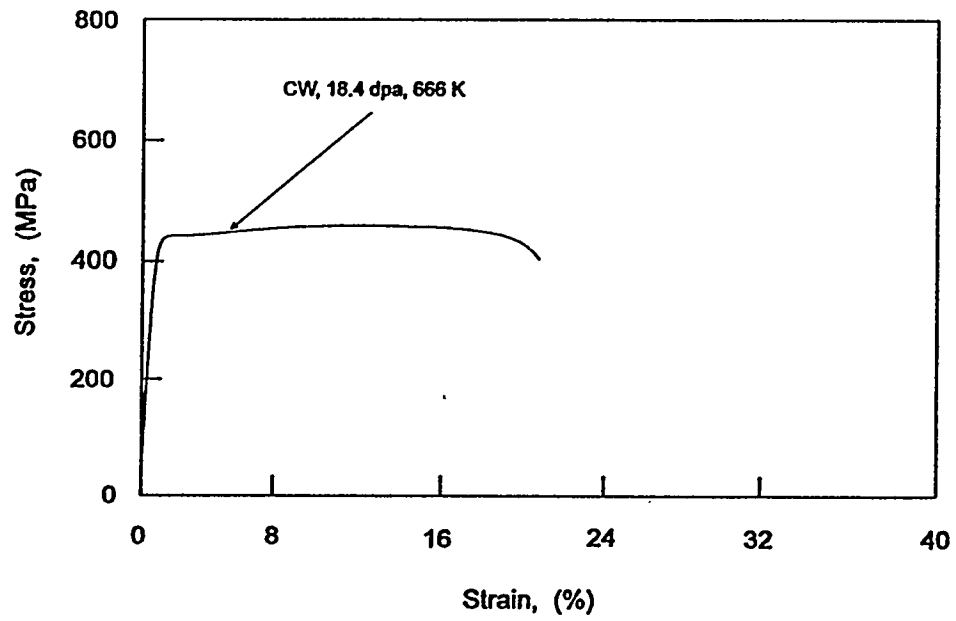


Figure 8a. Fractography of the unirradiated specimen 96% CW CuAl25. Note the presence of α - Al_2O_3 inclusions in some of the dimples.

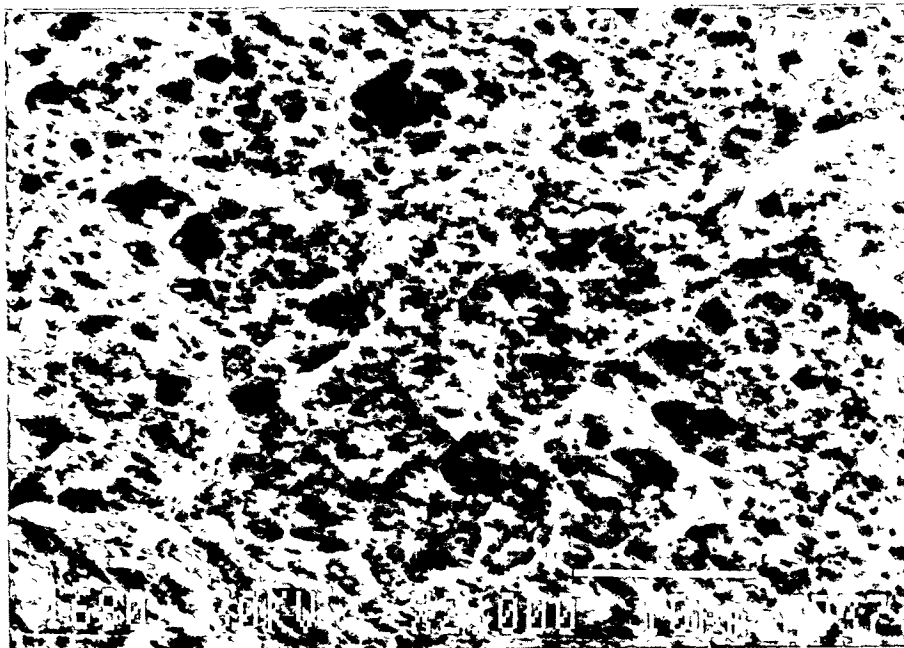
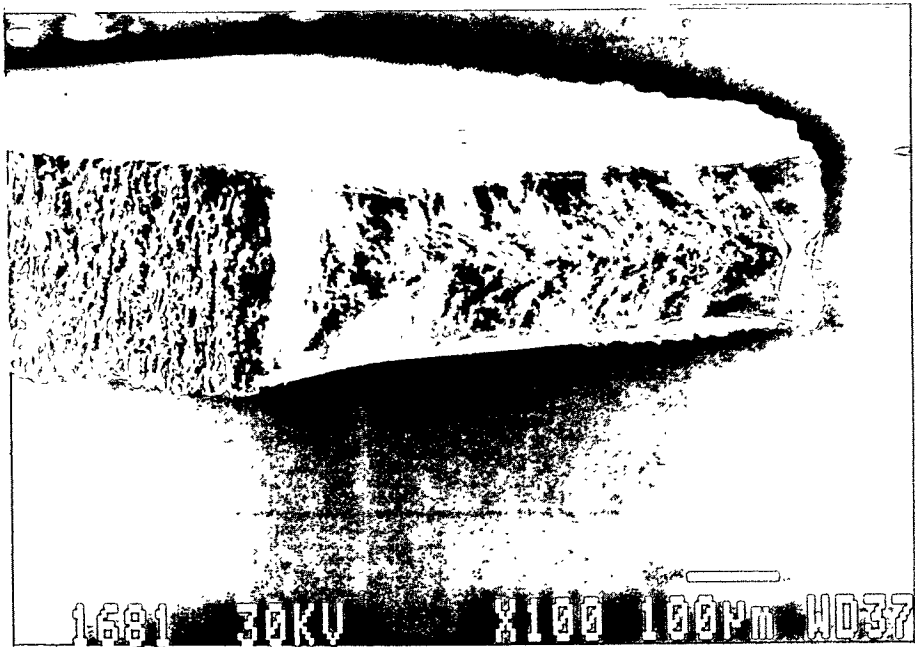


Figure 8b. Fractography of the irradiated specimen CW CuA125.

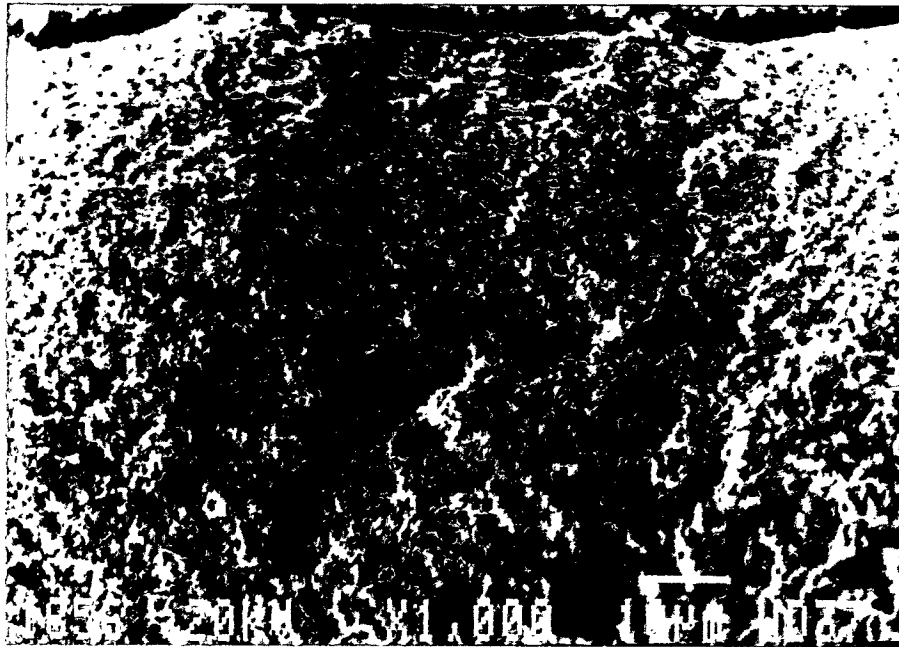
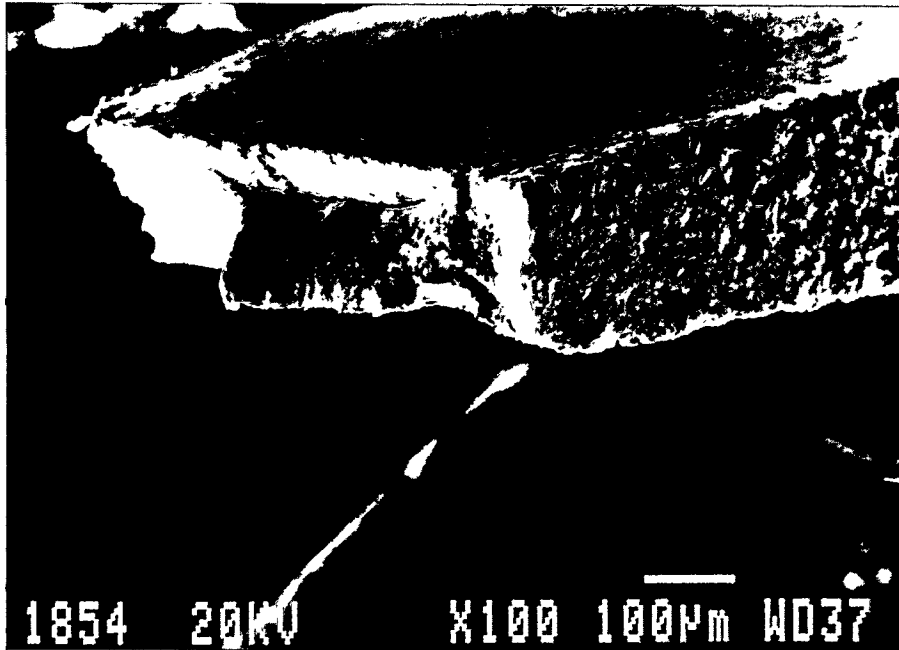


Figure 9a. Fractography of the unirradiated GlidCop-Nb alloys.

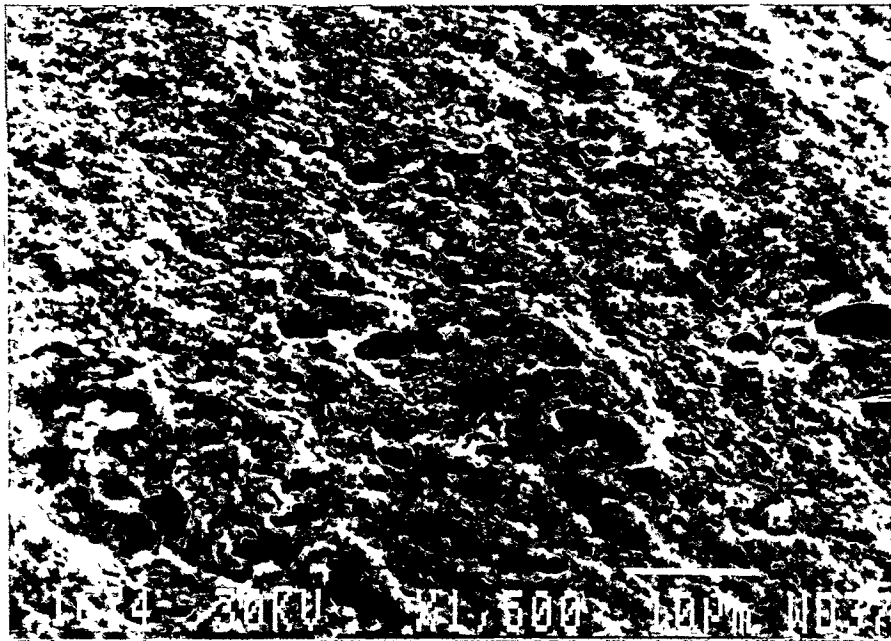
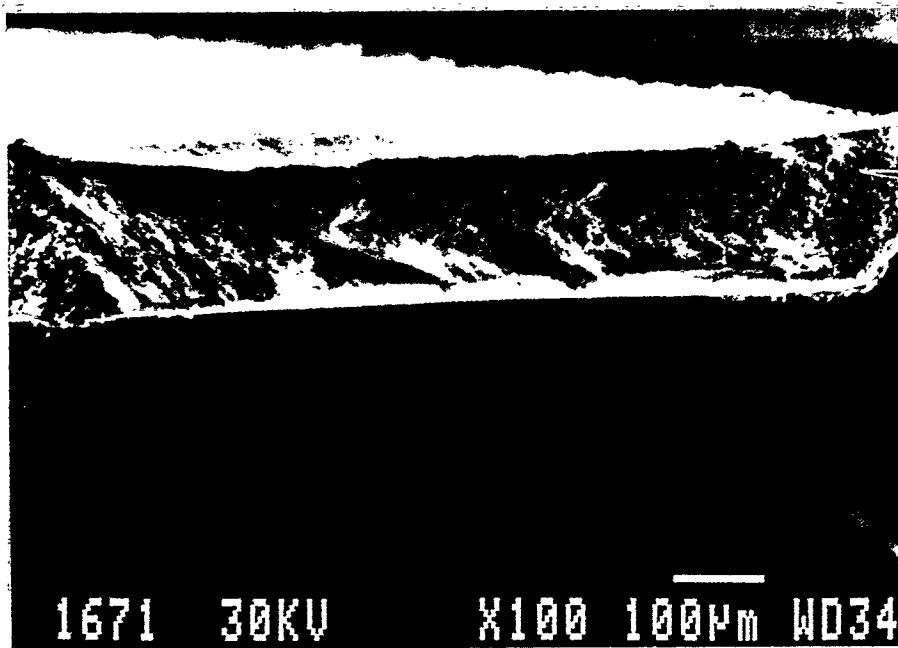


Figure 9b. Fractography of the irradiated GlidCop-Nb alloys.

